A Reanalysis of the Surface Winds for Hurricane Donna of 1960

JASON P. DUNION

NOAA/AOML/Hurricane Research Division and CIMAS, University of Miami, Miami, Florida

CHRISTOPHER W. LANDSEA, SAMUEL H. HOUSTON,* AND MARK D. POWELL

NOAA/AOML/Hurricane Research Division, Miami, Florida

(Manuscript received 7 March 2002, in final form 27 January 2003)

ABSTRACT

Hurricane Donna, the only major hurricane to strike the United States during the 1960 Atlantic hurricane season, passed over the middle Florida Keys near Sombrero Key before making landfall southeast of Naples, near Goodland, Florida, on 10 September at approximately 1600 UTC. This study makes detailed retrospective surface wind analyses of Hurricane Donna utilizing the National Oceanic and Atmospheric Administration (NOAA) Hurricane Research Division's (HRD) H*Wind surface wind analysis system. Analyses were produced at intervals of 6 h between 1800 UTC 9 September and 1200 UTC 11 September 1960 while the hurricane was close to and over Florida. These analyses depict the storm track as well as the distribution and extent of tropical storm force, 50 kt (25.7 m s^{-1}), and the hurricane-force wind radii throughout this time period and include new methodologies for adjusting aircraft flight-level data to the surface in the tropical cyclone core environment. Algorithms were developed to account for the effects of eyewall tilt and the warm core structure typical of tropical cyclones. Additional methods were developed using global positioning system (GPS) dropwindsondes (sondes) to more accurately adjust boundary layer winds to equivalent surface winds. The Kaplan–DeMaria Inland Wind Decay Model was also used for the first time to adjust landfall data being input into the H*Wind system. These data were used to generate low-weighted background fields that helped generate postlandfall wind field analyses of Hurricane Donna. Finally, swaths of peak winds, duration of hurricane- and major hurricane–force winds, and wind steadiness were produced to facilitate damage assessment. The information provided by these objective analyses is significantly more detailed than the more limited descriptions of peak winds, storm position, and minimum central pressure available in the National Hurricane Center's (NHC) hurricane database archive (HURDAT).

1. Introduction

Although major hurricanes (maximum 1-min sustained surface winds of $\geq$49 m s^{-1}) account for only 20% of all landfalling tropical storms and hurricanes, they account for over 80% of the tropical cyclone damages in the continental United States (Pielke and Landsea 1998).[1] This suggests the importance of improving our ability to accurately analyze and forecast these destructive storms. The current use of parametric simulations by catastrophe-modeling companies to describe a hurricane's landfall may be inadequate because of the simplifying assumptions inherent in their derivation (Pielke and Pielke 1997). This study describes reconstruction and mapping of surface wind speed, maximum 1-min sustained wind speeds, wind steadiness, and duration of peak winds for Hurricane Donna of 1960 that are based on observations and allow for direct comparison of catastrophe model output to observationally based analyses.

Hurricane Donna affected an extensive area of the southwestern Florida peninsula between 9 and 11 September 1960. The National Hurricane Center's hurricane database archive (HURDAT; Jarvinen et al. 1984) indicates that maximum 1-min sustained surface winds at landfall reached 64 m s^{-1} and storm surges of up to 4 m in the middle Florida Keys and near Lostman's River south of Naples, Florida, were reported (Dunn 1961). Destruction was severe from the combination of strong winds and flooding, particularly northeast of the storm track. Vast expanses of mangrove stands in western areas of Everglades National Park incurred losses that ranged from one-half to total destruction. The great

[1] This manuscript defines maximum 1-min sustained winds as a maximum in time occurring at a particular location. NOAA/NHC's definition refers to a maximum that occurs at a particular point in time only.

* Current affiliation: NOAA/National Weather Service Forecast Office/Central Pacific Hurricane Center, Honolulu, Hawaii.

Corresponding author address: Jason P. Dunion, NOAA/AOML/Hurricane Research Division, 4301 Rickenbacker Cswy., Miami, FL 33149.
E-mail: Jason.Dunion@noaa.gov

white heron population residing in the park at that time was decimated by 35%–40% (Tisdale 1960). Human fatalities and property losses associated with this storm were relatively low and can be partially attributed to the relatively low population density in the region at that time. However, because of the dramatic increase of infrastructure and population in south Florida since 1960, estimates of the total damage that Hurricane Donna would inflict on the region today are on the order of $12 billion (Pielke and Landsea 1998). The reader is referred to Tisdale (1960) for a comprehensive discussion of Hurricane Donna's synoptic history and strom track.

The maximum surface winds associated with this tropical cyclone as it moved toward the Florida peninsula were largely based on observations from reconnaissance aircraft. Miller (1963, 1964) examined the filling of Donna as its circulation encountered the southwest Florida peninsula. Houston and Powell (2003; manuscript submitted to *J. Coastal Res.*, hereafter HP3) examined the winds fields of Hurricane Donna over water, prior to its landfall over southwest Florida. These wind fields were used primarily for examining hydrologic aspects of the storm, but were also used for comparisons with ecological damages observed in Florida Bay, the Florida Keys, and along the southwest Florida peninsula. However, the extent and distribution of surface winds associated with this landfalling hurricane have not been extensively documented. Detailed surface wind analyses provide additional insights into Hurricane Donna's structure that were not addressed by Dunn (1961), Tisdale (1960), or HP3. This study first discusses conventional techniques for adjusting aircraft flight-level winds to the surface and subsequently introduces new procedures for adjusting these winds to the surface (section 2). Later sections examine the structure and evolution of Hurricane Donna's wind field before and after its landfall near Naples, Florida.

2. Procedure

a. Conventional surface adjustment of flight-level data

Flight-level reconnaissance and research data are a critical component to generating accurate surface wind analyses. This is often the only data available for directly describing the winds in the tropical cyclone core. Flight-level data (811 hPa) from the National Hurricane Research Project (NHRP) provided the main component of the core data, while U. S. Navy reconnaissance flight-level data (700 hPa) were gathered in mainly peripheral areas of Donna. Navy aircraft were focused on gathering position estimates from radar for this storm and did not make any eyewall penetrations during the time scope considered in this study.

The adjustment of the flight-level data to the surface was necessary to generate surface winds for analysis since, as is common for nearly all landfalling hurricanes, little in situ surface data were available under the eyewall. Initially, procedures described by Powell and Houston (1996) were followed, mirroring the process that is conducted by National Oceanic and Atmospheric Administration's (NOAA)'s Hurricane Research Division, (HRD) in current experimental real-time surface wind analysis operations. The methods of Powell et al. (1996) were used to generate 10-m, maximum 1-min. sustained winds valid for marine exposure. This methodology involves a two-step adjustment process to convert flight-level winds to equivalent surface winds. First, flight-level winds are assumed to roughly correspond with wind speeds and directions found in the mean boundary layer (MBL), defined as the average wind conditions in the lowest 500 m of the atmosphere. Next, these MBL winds are converted to surface winds surface similarity theory as a framework for the adjustment process. The surface to MBL wind speed ratio is a function of both the air–sea temperature difference and MBL wind speed. For standard tropical atmospheric–oceanic conditions (i.e., $T_{\mathrm{Atm}} - T_{\mathrm{SST}} = -3.5°\mathrm{C}$), the ratio varies from 0.9 for a MBL wind speed of 29 m s^{-1} to 0.8 at 70 m s^{-1}. The estimate utilized for the air–sea temperature difference is consistent with values found in tropical cyclone environments by Cione et al. (2000). A directional backing of 20° is applied to wind vectors to account for frictional effects inherent in the surface adjustment process.

b. New methodologies for equating aircraft flight-level winds to MBL winds

Recent data from global positioning system (GPS) dropwindsondes (sondes; Hock and Franklin 1999) in tropical cyclone environments suggest that additional factors need to be considered in the surface adjustment process currently employed by HRD, particularly in high-wind (>55 m s^{-1}) regimes and areas in the storm core (Franklin et al. 2000; Powell et al. 1999). GPS sondes (launched from NOAA research and U.S. Air Force reconnaissance aircraft) measure wind data in the tropical cyclone environment, providing wind speed accuracies of 0.5–2 m s^{-1} and vertical resolutions of approximately 5 m (Hock and Franklin 1999). Winds measured by the GPS sonde represent instantaneous quasi-Lagrangian measurements. A total of 280 TC inner core GPS sondes were available at the time of this study. Many of these 280 GPS sondes were launched from below 700 hPa, therefore limiting the size of that dataset relative to the 850-hPa and 500-m levels. To maintain consistency, only the 185 GPS sondes that contained complete data from 700 hPa, 850 hPa, and 500 m were utilized to determine the flight-level–MBL wind speed relationships.

Figure 1 addresses the first assumption made by HRD's planetary boundary layer (PBL) model: the supposition that, regardless of altitude, wind speeds mea-

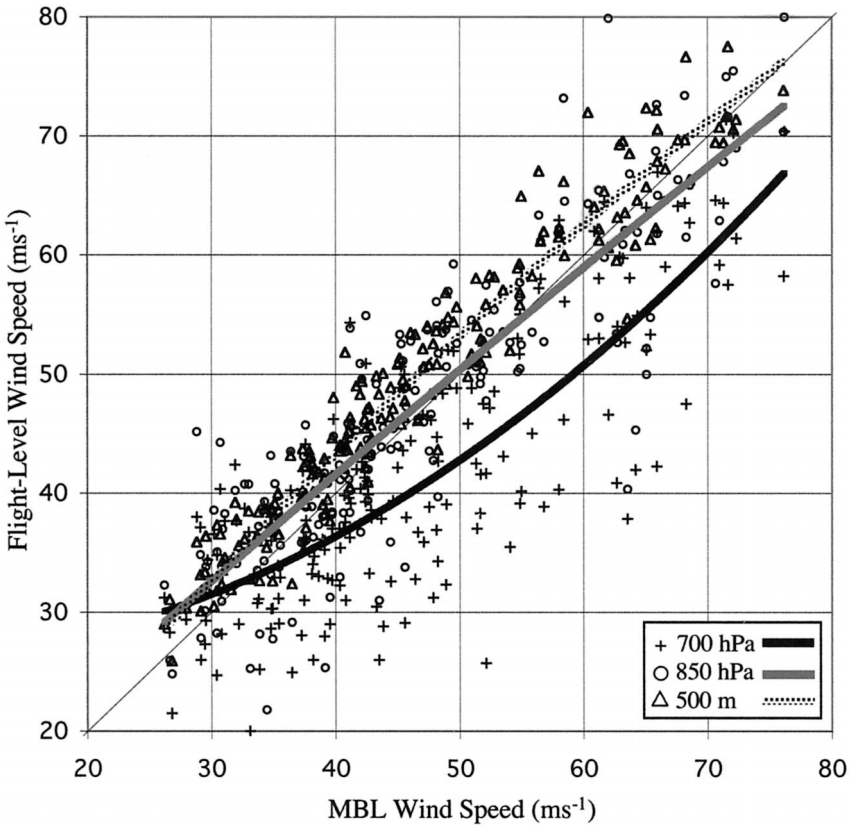

FIG. 1. Scatterplot of MBL winds vs winds at three typical reconnaissance aircraft flight levels based on data from 185 GPS sondes dropped in several tropical cyclone core regions. The curves indicate second-order polynomial best fits to the data.

sured by reconnaissance aircraft are equivalent to MBL winds. This plot was generated using data from GPS sondes launched in the core regions of several tropical cyclones during the 1998 and 1999 Atlantic and northeast Pacific hurricane seasons (see Table 1) and shows the correlation between MBL wind speeds and winds from various flight-level altitudes. In this case, the *core region* was defined by

$$\frac{R_{\mathrm{GPS}}}{\mathrm{RMW}} < 2.0, \tag{1}$$

where R_{GPS} represents the radius of the GPS sonde launch point from the storm center and RMW is the radius of the maximum flight-level wind from the storm center.

TABLE 1. GPS sonde core region data utilized for this study. Tropical cyclone, launch platform used (U.S. Air Force or NOAA), flight dates, and number of GPS sondes utilized are indicated.

Tropical cyclone	Aircraft platform	Date	No. of sondes
Bonnie	AF/NOAA	21–26 Aug 1998	95
Bret	AF/NOAA	21–22 Aug 1999	8
Danielle	AF	27–31 Aug 1998	3
Dennis	AF	26 Aug–4 Sep 1999	25
Dora	AF	15–18 Aug 1999	6
Erika	NOAA	7–8 Sep 1997	18
Eugene	AF	12 Aug 1999	2
Floyd	AF/NOAA	9–15 Sep 1999	46
Georges	AF/NOAA	19–27 Sep 1998	21
Gert	AF	16–21 Sep 1999	4
Guillermo	NOAA	3 Aug 1997	2
Irene	AF	18 Oct 1999	1
Jose	AF	20 Oct 1999	1
Lenny	AF	15–19 Nov 1999	12
Mitch	AF/NOAA	24–29 Oct 1998	26

United States Air Force reconnaissance missions typically involve predetermined flight levels, dictated by a storm's intensity. Weaker tropical storms and depressions are usually flown at 500 m, while more intense tropical cyclones are flown at 850 or 700 hPa for safety reasons (OFCM 2002). Although GPS sonde data in Fig. 1 show that 500-m and 850-hPa flight-level winds correspond well to MBL winds in the core (generally less than 5% difference), 700-hPa wind speeds are consistently slower, particularly in MBL wind speed regimes above 30 m s^{-1}. A possible explanation for this tendency is the fact that stronger storms typically contain a warm core region that extends below 700 hPa that acts to lower the atmospheric pressure gradient and hence decrease the winds above the boundary layer (Hawkins and Rubsam 1968). This phenomenon, coupled with the effects

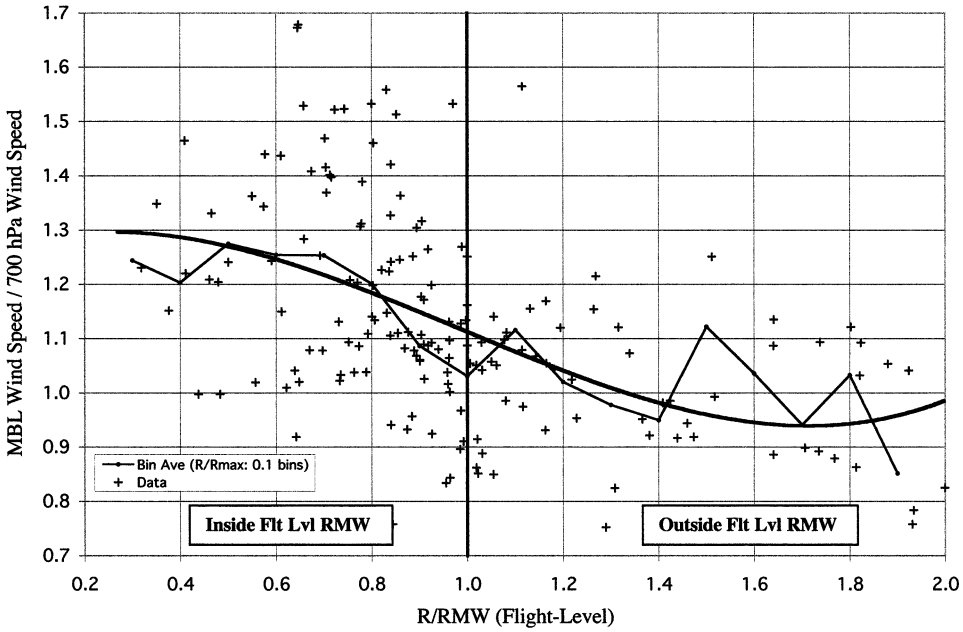

FIG. 2. Scatterplot and best-fit curve for the warm core–eyewall tilt correction. The relationship of the 700-hPa wind speed to the MBL wind speed as a function of proximity to the RMW is shown.

of eyewall tilt in the core of a tropical cyclone, complicate the conversion of flight-level to MBL winds and necessitate stratification by distance from the storm center with respect to the RMW at flight level. This approach was also examined by Franklin et al. (2000).

Eyewall tilt refers to the vertical tilting of the convective eyewall region of a tropical cyclone (TC). This phenomenon has been documented using aircraft-based Doppler velocity radar studies (e.g., Marks et al. 1992). Since the eyewall in well-developed TCs is usually tilted in the vertical and not oriented perpendicularly to the surface, the ratio of the MBL wind to the flight-level wind is dependent on the radius from storm center, as well as the actual flight level. Figure 1 statistically indicates that 500-m and 850-hPa flight levels are low enough in altitude such that the enhancement of winds by the warm core is being balanced by frictional effects in the boundary layer. However, 700-hPa flights are high enough to cause the MBL and flight-level wind speeds to be inconsistent. Using data from the 185 GPS sondes, an empirical adjustment was created to convert 700-hPa flight-level wind speeds to equivalent MBL winds. This adjustment uses a ratio of the radius from storm center of the flight-level observation and the RMW observed at flight level and allows for the normalization of tropical cyclone size. This empirical adjustment helps improve the algorithm's utility such that it can be applied to tropical cyclones of various sizes and intensities.

Figure 2 shows the relationships between the previously mentioned speed ratio and the MBL–700-hPa wind speed ratio. This plot indicates that the conversion of 700-hPa winds to MBL winds requires a speed boosting, particularly near or inside of the RMW (R/RMW < 1.3). At the RMW, boosts to 700-hPa winds of approximately 10% are indicated. In areas well outside of the flight-level RMW, the 700-hPa wind speeds require minor reductions to be properly converted to MBL winds. The adjustment of a 700-hPa flight-level wind speed (U_{700}) to an equivalent MBL wind (U_{MBL}) is represented by a third-order polynomial given as

$$U_{\mathrm{MBL}} = U_{700}\left[2.31 \times 10^{-1}\left(\frac{R}{\mathrm{RMW}}\right)^{3} - 6.82 \times 10^{-1}\left(\frac{R}{\mathrm{RMW}}\right)^{2} + 3.04 \times 10^{-1}\left(\frac{R}{\mathrm{RMW}}\right) + 1.26\right], \quad (2)$$

where R is the radius from the circulation center of the observed flight-level wind. The warm core–eyewall tilt adjustment indicated in Eq. (2) is only applicable to winds speeds measured at altitudes between 650 and 750 hPa and when R/RMW ≤ 2.0 and ≥ 0.25. A boost of 30% is recommended when R/RMW < 0.25.

Figures 1 and 2 indicate that the current assumption by the HRD PBL model that 700-hPa flight-level wind speeds are equivalent to values found in the MBL needs to be reexamined. Figure 3 again shows the relationship between MBL and 700-hPa winds as measured by 185 GPS sondes and indicates that uncorrected, the 700-hPa winds (black curve) are consistently slower than the MBL wind. The gray curve shows that the MBL–700-hPa wind correlation is markedly improved by the application of the warm core–eyewall tilt correction term

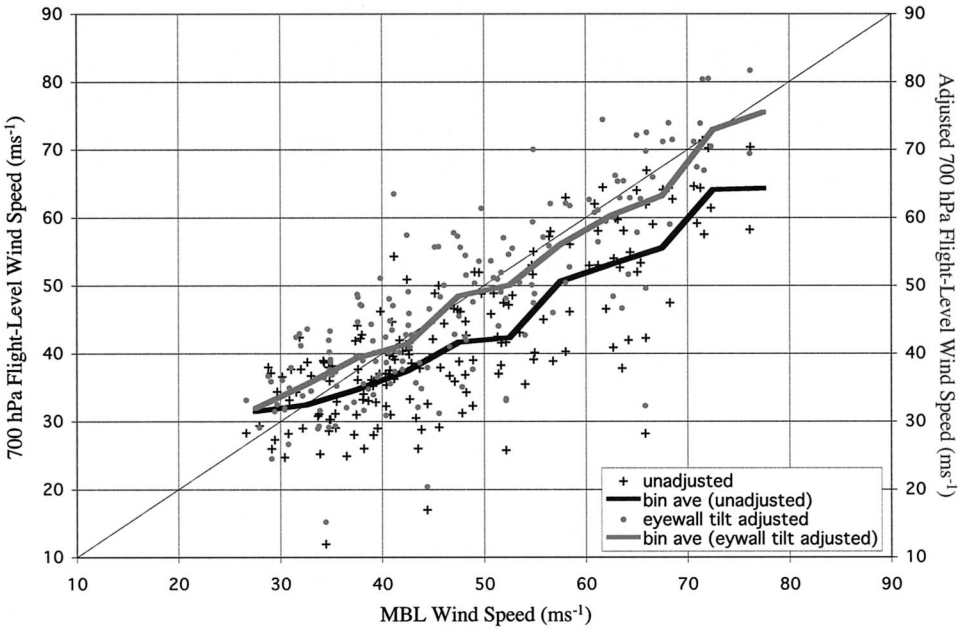

FIG. 3. Scatterplot and binned averages of MBL vs 700-hPa-level wind speeds. Unadjusted 700-hPa winds are indicated in black and are consistently slower than the MBL wind. Here, 700-hPa-level winds that have been warm core–eyewall tilt adjusted according to the recommendations in Fig. 2 are shown in gray and indicate correlation improvements.

given in Eq. (2) and quantified in Table 2. Based on the dependent GPS sonde dataset, the uncertainty of the flight-level to MBL adjustment method is ~13%.[2]

After improvements were made in the methodology for converting flight-level winds to equivalent MBL winds, attempts were then made to ascertain the quality of the conversion process by the HRD PBL model of MBL winds to surface winds.

c. New methodologies for equating MBL winds to surface winds

The adjustment of MBL wind speeds to equivalent maximum 1-min sustained surface winds (10-m elevation) with marine exposure is calculated by HRD's PBL model and involves an iterative process that employs surface-layer similarity theory. Verification of the quality of this adjustment scheme was difficult in the past, given the formidable task of capturing coincident flight-level data with precise, 10-m surface wind data in the tropical cyclone core (Powell and Black 1990). GPS sondes now provide an effective tool for examining the boundary layer wind structure in the TC environment, as well as for verifying HRD's surface adjustment process.

Using 280 GPS sondes dropped in tropical cyclone environments (see Table 1) statistics were generated to relate MBL wind speeds to those at the surface. A *surface wind* was defined as a 10-m wind with marine exposure and only GPS sondes that reported data within 30 m of this level were accepted into the statistics. Those sondes that did not report an exact 10-m wind speed were adjusted to an equivalent 10-m wind using an empirically derived algorithm based on data from 122 inner core GPS sondes. This adjustment is applicable to winds at or below 50-m height and is shown by the solid curve in Fig. 4 and is given by

$$U_{\text{sfc}} = U_z\{-0.0703\ [\text{Ln}(Z) + 1.1651]\}, \qquad (3)$$

where U_{sfc} and U_z are the wind speeds at 10 m and at height, Z, respectively. GPS sondes that did not report a wind within the lowest 30 m above the surface or did not record sufficient data within the lowest 0–500 m to calculate a MBL wind speed were omitted from the statistics. Figure 4 also shows the equivalent surface adjustment for near-surface winds based on a standard logarithmic profile using the Charnock (1955) relation-

TABLE 2. Comparison between the original assumption that MBL and 700-hPa flight-level wind speeds are equivalent and the proposed new method that accounts for warm core–eyewall tilt effects on this relationship (based on dependent data).

	MBL vs 700-hPa flight-level wind (original assumption)	MBL vs 700-hPa flight-level wind (new method)
Correlation coefficient	0.77	0.82
Rmse (m s^{-1})	9.8	7.6
700-hPa bias (m s^{-1})	−5.5	−0.1

[2] This adjustment was developed using data collected in the inner cores of mature TCs with well-defined eyewall structures. It may not be applicable to TCs lacking well-developed eyewall structures.

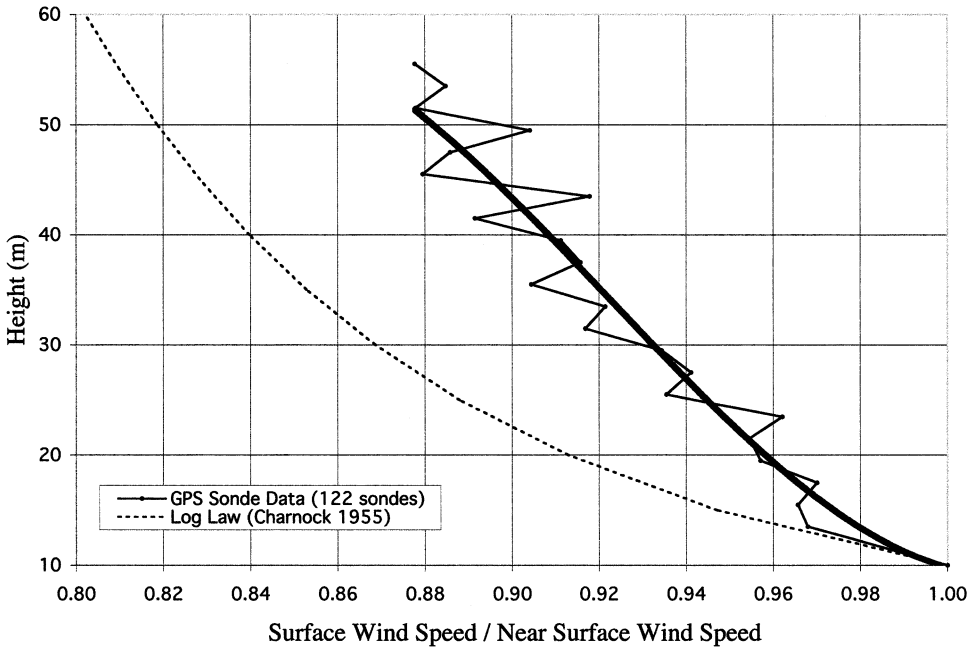

FIG. 4. Plot of surface–near-surface wind speed ratios vs height. The solid curve was generated from 122 GPS sondes dropped in various TC core regions, using a bin size of 2 m in the vertical. This plot and overlaid best-fit curve indicate that the use of a traditional logarithmic surface adjustment (dashed curve) based on assumptions by Charnock (1955) produces excessively slow surface winds in the TC environment.

ship for roughness length. This log profile exhibits a negative bias when compared with the GPS statistics. This suggests that current methodologies that assume a conventional logarithmic-based surface adjustment scheme in TC environments are overestimating marine roughness lengths, particularly in extreme wind regimes.

Figure 5 shows various relationships between the

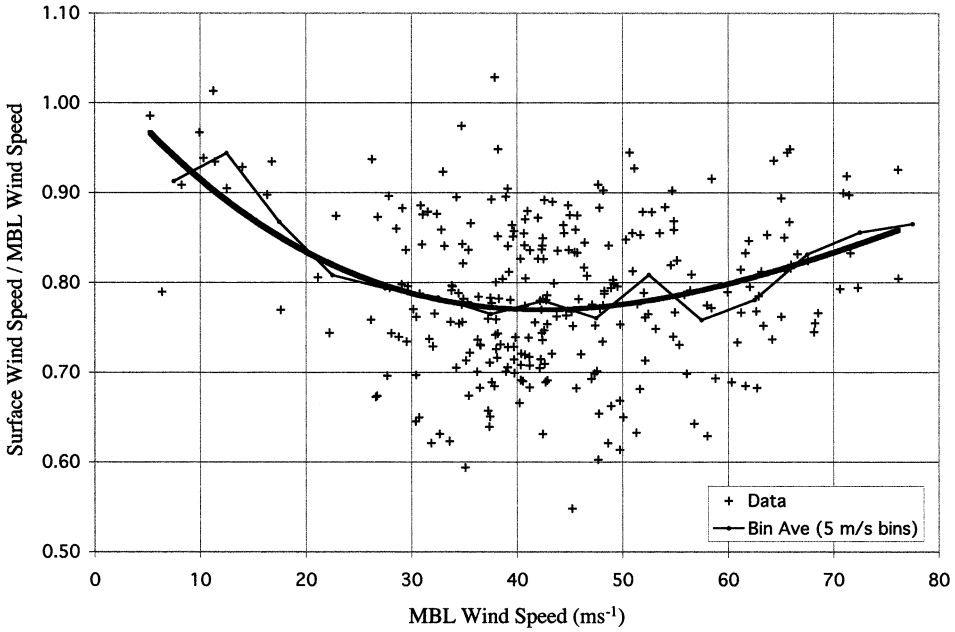

FIG. 5. Scatterplot and best-fit curve showing the relationship between MBL (0–500 m) and surface (10 m) wind speeds as determined from 280 GPS sondes dropped in TC core environments. A nonlinear, wind speed–dependent relationship is indicated.

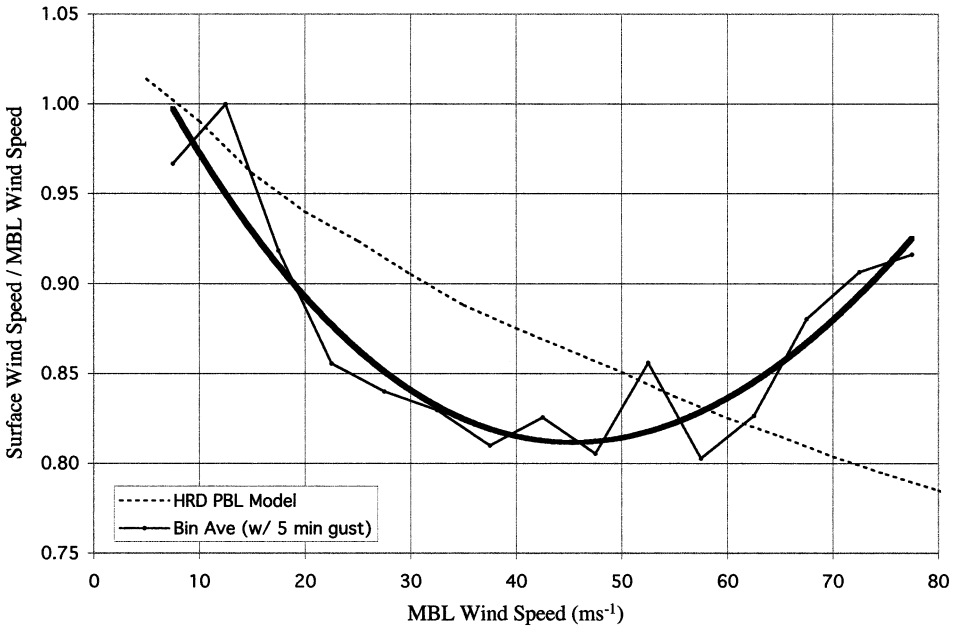

FIG. 6. Mean binned average (5 m s^{-1} bins) and overlaid best-fit curve (solid black lines) showing the relationship between surface (10 m) and MBL (0–500 m) wind speeds as determined from 280 GPS sondes dropped in TC core environments. The HRD PBL model (dashed black line).

MBL wind speed and the equivalent 10-m surface wind speed as determined from 280 GPS sondes. The scatter of the data indicates that this relationship is highly variable, making it difficult to make broad generalizations. This partly relates to the temporal differences between the GPS sonde surface wind (instantaneous) and the GPS sonde MBL wind (~35–45 s). However, a relationship does appear to exist within the data, which suggests that the surface wind is dependent on the magnitude of the MBL wind speed. The black curve shows the data grouped into 5 m s^{-1} bins and indicates that a nonlinear relationship exists between various MBL and surface wind speeds. This MBL to surface wind relationship is based on a fit to numerous GPS sonde observations and therefore represents a mean condition. There is no basis for assuming that a mean condition should be representative of a maximum 1-min sustained wind value. Hence, we make the assumption that the mean condition represents a 5-min mean. For example, in adjusting tropical cyclone mean boundary layer model winds to equivalent surface winds, assumptions of 1 h (Vickery and Twisdale 1995) or 20–30 min (Thompson and Cardone 1996) have been used. Our assumption of a 5-min value is based on comparisons of surface winds estimated from GPS sonde MBL winds and NOAA marine platforms (Houston et al. 2000; S. H. Houston 2000, personal communication). The best comparisons were achieved when a 5-min mean was assumed. The gust factor adjustment is discussed in detail by Powell et al. (1996) and can be described by a third-order polynomial:

$$G_{60,T} = 2.6631 - 2.1244(\log_{10}T) + 0.85245(\log_{10}T)^2 - 0.10346(\log_{10}T)^3, \quad (4)$$

where T represents the averaging period (s) to convert from and usually results in a boosting of the wind. A 5-min (300 s) wind requires an additional boost of 1.059 to attain an equivalent maximum 1-min sustained wind and was applied to the best-fit curve in Fig. 6. The dashed black curve shows the surface–MBL wind speed ratios is calculated by HRD's PBL model, assuming

TABLE 3. Mean sea level pressure (MSLP), peak wind, RMW (surface), and significant wind radii estimates from HURDAT and H*Wind reanalyses for Hurricane Donna (prelandfall/landfall).

Date	MSLP (hPa)	Peak wind HURDAT (kt/m s^{-1})	Peak wind H*Wind (kt/m s^{-1})	RMW H*Wind (km)	34-kt radii NE/SE/SW/NW (km)	50-kt radii NE/SE/SW/NW (km)	64-kt radii NE/SE/SW/NW (km)
1800 UTC 9 Sep 1960	939	125/64	117/60	30	248/254/237/246	178/146/159/191	117/117/57/131
0000 UTC 10 Sep 1960	932	120/62	117/60	30	257/213/211/222	172/124/144/180	128/94/106/135
0600 UTC 10 Sep 1960 (Florida Keys)	932	115/59	117/60	33	248/185/174/200	128/111/111/143	94/80/74/117
1200 UTC 10 Sep 1960	938	120/62	107/55	33	226/180/152/154	143/133/91/107	67/78/63/78
1600 UTC 10 Sep 1960 (Naples)	—	120/62	98/50	33	215/185/157/141	93/94/85/106	63/59/57/74

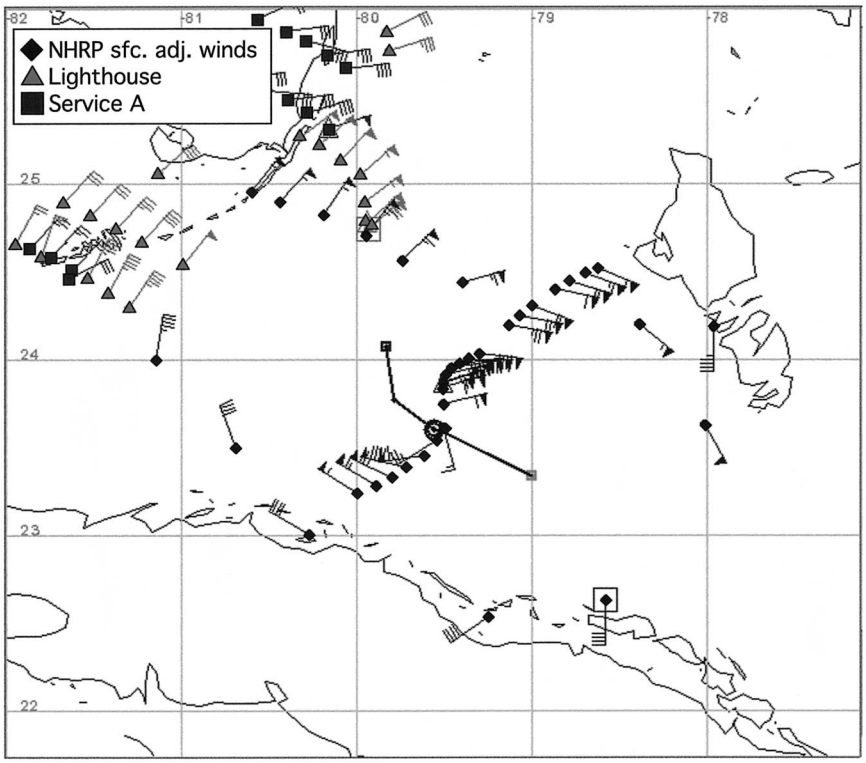

FIG. 7. Observations used in the prelandfall Hurricane Donna surface wind analysis for 1800 UTC 9 Sep 1960. Winds are max 1-min sustained 10-m surface winds valid for marine exposure. The data are plotted in storm-relative coordinates with a time window of ±4 h from the analysis time. Observations enclosed by square (triangle) symbols indicate the latest available observation (max obs wind speed) per platform type.

unstable conditions with an air–sea temperature difference of −3.5 C.[3] This curve shows that as the MBL wind speed increases, the computed surface winds speed ratio steadily decreases. This trend is partially related to the PBL model's calculation of roughness length, which increases with increasing wind speed and acts to further reduce the compound surface wind. The solid curve indicates surface to MBL wind speed ratios (separated into 5 m s^{-1} MBL wind speed bins) as determined by the 280 GPS sondes. These ratios include the application of a 5-min gust factor adjustment to the calculated surface reduction ratios in order to generate an equivalent maximum 1-min sustained wind. The GPS data suggest that HRD's PBL model performs reasonably well in MBL wind speed regimes of up to 55 m s^{-1}. Above this threshold, the model appears to underestimate the equivalent surface wind on average, which was also suggested in work done by Powell et al. (1999). This study utilized the HRD PBL model to make MBL to surface wind adjustments, unless the calculated MBL wind reached or exceeded 55 m s^{-1}, at which point statistics based upon the GPS sonde data (represented by a third-order polynomial) were used (see Fig. 6):

$$U_{\text{sfc}} = U_{\text{MBL}}[(-2.84 \times 10^{-7})U_{\text{MBL}}^3 + (1.58 \times 10^{-4})U_{\text{MBL}}^2 - (1.25 \times 10^{-2})U_{\text{MBL}} + 1.08], \quad (5)$$

where U_{MBL} represents the MBL wind speed and U_{sfc} is the equivalent 10-m surface wind speed. The relatively few number of GPS sondes that reported MBL winds above 72 m s^{-1} dictated that a surface wind ratio of no more than 90% be utilized in these high wind regimes. This quantity may change by 5%, since additional work is proceeding to gather GPS sonde wind speed data in these extreme wind regimes. Based on the dependent GPS sonde dataset, the uncertainty of the MBL to surface adjustment method is ~7%. This dataset (shown in Table 1) does contain a significant number of sondes dropped in Hurricane Bonnie of 1998. Though this storm exhibited below-normal flight-level to surface wind speed ratios, the 700-hPa flight-level winds averaged only 38 m s^{-1} and do not significantly impact the MBL–surface high wind speed (>55 m s^{-1}) statistics.

[3] This model assumes warm SSTs with unstable conditions and may not be applicable to TCs located over cold SSTs and stable conditions.

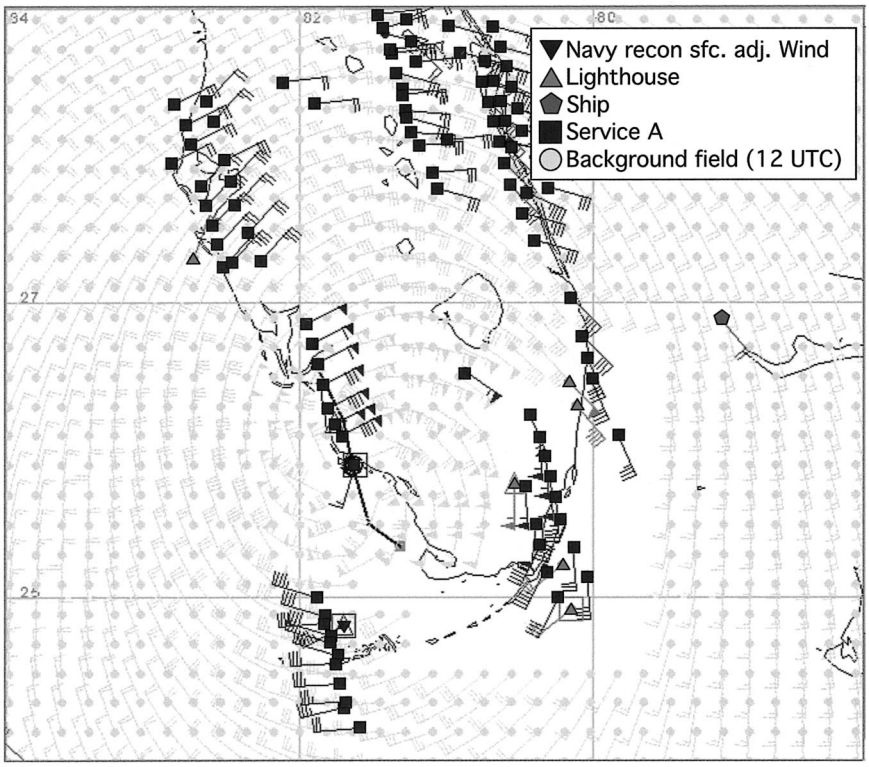

FIG. 8. The same as in Fig. 7 except for observations used in the landfall Hurricane Donna surface wind analysis for 1600 UTC 10 Sep 1960.

3. Surface wind analyses of Hurricane Donna

*a. HRD's surface wind analysis system (H*Wind)*

HRD currently provides the National Hurricane Center (NHC) with objective tropical cyclone surface wind analyses in real time for use as guidance in the determination of tropical cyclone wind field distributions, particularly the extent of the tropical storm and hurricane-force winds (Powell et al. 1998). H*Wind takes in situ and remotely sensed wind data as input and generates isotach and streamline analyses. This is accomplished using the Spectral Application of Finite-Element Representation (SAFER) method (Ooyama 1987; Franklin et al. 1993). This method uses cubic B-splines to minimize the differences between the input observations and the analysis. The isotachs are valid for both marine and overland (open terrain) exposure and are contoured using a land-masking feature that allows for a more comprehensive wind field generation at landfall. The investigations of historical tropical cyclones like Donna often pose a challenge because of relatively sparse data coverage by today's standards. Aircraft reconnaissance data were not as readily available for these storms due to the fewer number of inner core flights in that era. These older storms also predate the moored buoy and Coastal Marine Automated Network stations (C-MANs) first constructed in the 1970s. Finally, satellite observations that are readily available today, such as satellite cloud drift (Dunion and Velden 2002) and microwave scatterometer winds (Goodberlet et al. 1989; Katsaros et al. 2001) were unrealized technologies over 40 yr ago. Given the period and available technology, however, analyses of Hurricane Donna were made with a relatively large amount of wind data.

*b. Available data for H*Wind analysis*

The analysis of Hurricane Donna was made utilizing wind data from several platform types. The data collected for these analyses were recently described by HP3, who conducted similar analyses of winds for marine exposures exclusively. Reconnaissance aircraft data from research missions conducted by NHRP, as well as from navy reconnaissance missions, provided the bulk of inner core wind data in Donna prior to landfall. These observations were adjusted to the surface using the methods previously described. Ship data were available for analysis, as were surface reports from meteorological offices, military bases, and airports. These Service A observations were adjusted to 10 m based on archived station information (U.S. Department of Energy 1978) and then converted to equivalent marine-exposed winds before being input

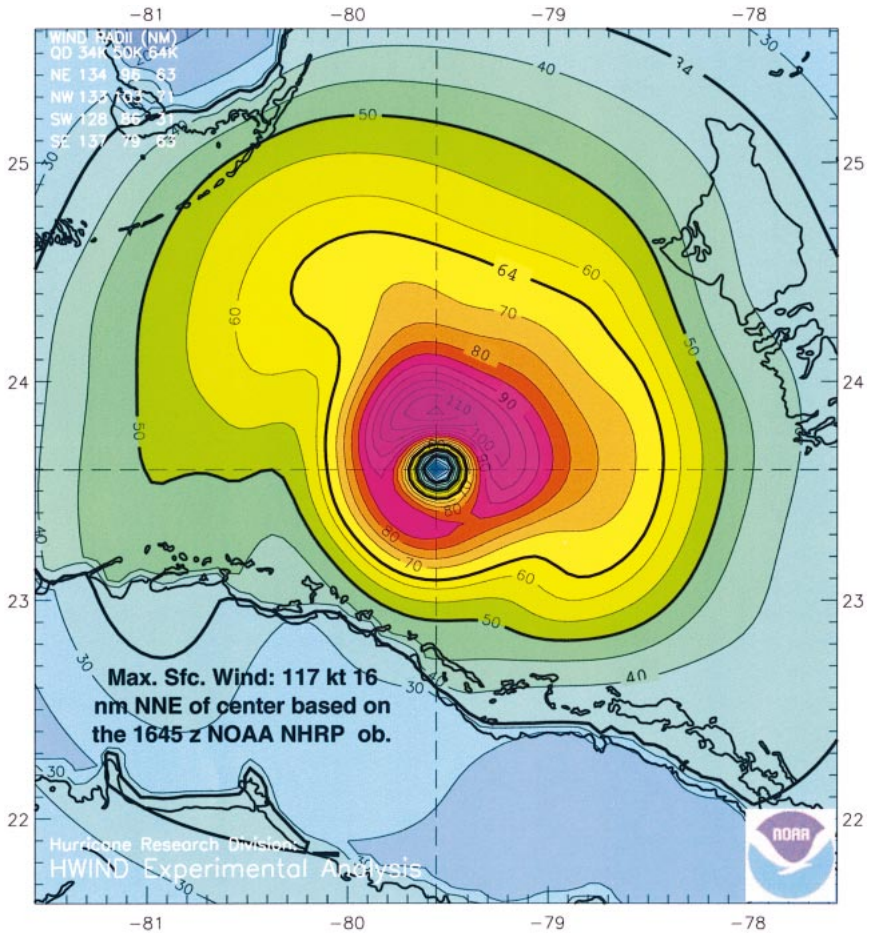

FIG. 9. Hurricane Donna prelandfall surface wind analysis for 1800 UTC 9 Sep 1960. Winds are max 1-min sustained 10-m surface winds (kt) valid for both marine and open terrain exposures. Significant wind radii are indicated in the upper-left corner. The analysis is based on NHRP flight-level winds adjusted to the surface from 811 hPa (1459–2027 UTC), as well as ship, lighthouse, and Service A surface reports (1400–2200 UTC).

into the H*Wind system.[4] This allowed for the H*Wind land-masking algorithms to correctly adjust these winds for exposure in a storm relative coordinate system. Lighthouse stations along the south Florida coast and Florida Keys provided the highest quality data, due to their preferable marine exposure. Specific attention was given to the reported observation times of the various surface stations. Although some stations recorded their meteorological data using universal time coordinated (UTC), many referenced local time in their reports. Since the Uniform Time Act that formalized the use of daylight savings time (DST) was not enacted until 1966, time zone inconsistencies existed throughout many states, including Florida. A reference guide that specifies the historic geographic use of DST was employed for this reconstruction work of Hurricane Donna (Duane 1985).

All observations for the Donna analyses were quality controlled and adjusted for height, exposure, and averaging time before being input into H*Wind. To stabilize the H*Wind runs, data from previous analyses were utilized as background fields for subsequent analyses. H*Wind surface wind analysis were made of Hurricane Donna from 1800 UTC 9 September and carried though to 1200 UTC 11 September 1960. Since the NHC best track only provides storm positions in 6-hourly increments, a more detailed track for Donna was reconstructed using a combination of best track position data and positions determined by reconnaissance aircraft radar. Data availability and resource constraints dictated that analyses be provided in 6-hourly increments throughout this study, with the exception of the addition of the 1600 UTC 11 September Naples landfall analysis. The 6-hourly analysis interval also matches the incre-

[4] Service A stations provided hourly meteorological information at airport locations. This data was disseminated to local forecast offices via teletype circuits. Meteorological Terminal Air Report (METAR) stations in use today are similar to this early network of observing stations.

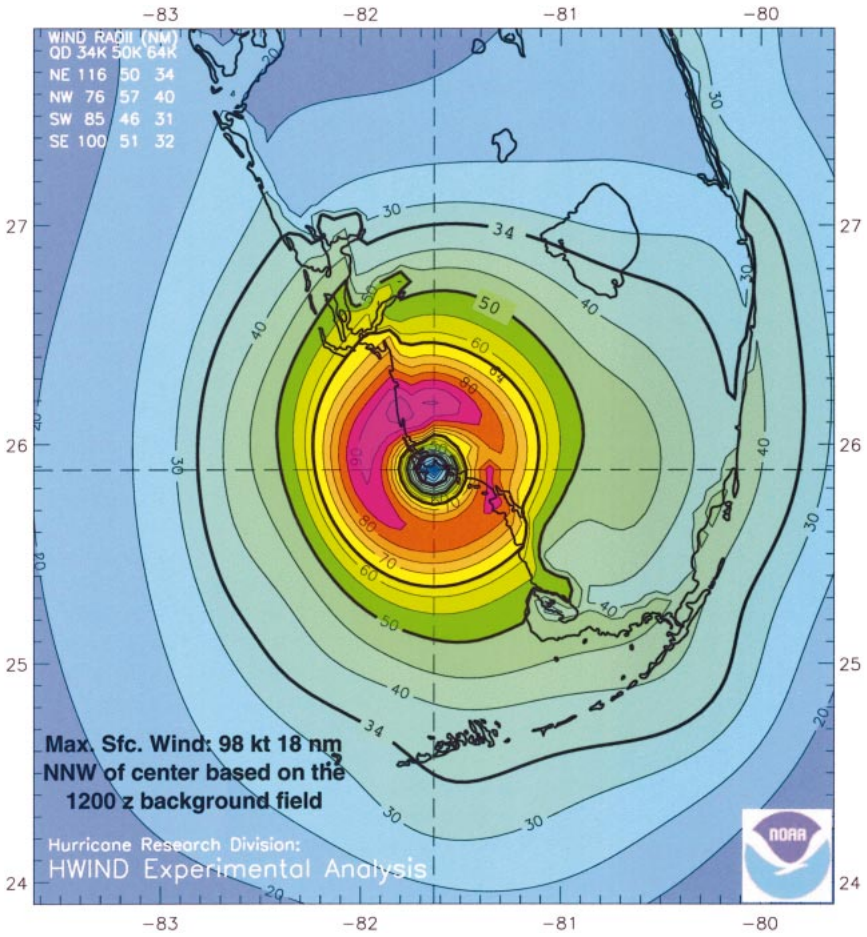

FIG. 10. Hurricane Donna landfall surface wind analysis for 1600 UTC 10 Sep 1960. Winds are max 1-min sustained 10-m surface winds (kt) valid for both marine and open terrain exposures. Significant wind radii are indicated in the upper-left corner. The analysis is based on background field data from the previous 1200 UTC analysis, U.S. Navy reconnaissance flight-level winds adjusted to the surface from 700 hPa (1930 UTC), as well as ship, lighthouse, and Service A surface reports (1200–1800 UTC).

ment between position–intensity estimates in the best track database.[5]

c. *Prelandfall surface wind analyses of Hurricane Donna*

Five surface wind analyses were made of Hurricane Donna beginning 1800 UTC 9 September 1960 up to and including the time it made landfall near Naples, Florida, on 1600 UTC 10 September 1960. Donna made a first landfall in the middle Florida Keys near Sombrero Key around 0600 UTC on 10 September. HURDAT indicates that Donna maintained itself as a category-4 hurricane on the Saffir–Simpson hurricane scale throughout this 22-h period. The reanalyses conducted in this study produced slightly lower winds than are indicated in HURDAT, but compare reasonably well (see Table 3). Maximum sustained winds estimated for Hurricane Donna by H*Wind analyses made during this prelandfall time period are based on surface-adjusted NHRP reconnaissance aircraft data. NHRP conducted its last flight into Donna on 9 September 1960 and measured a maximum flight-level (811 hPa) wind of 68 m s^{-1} at 1645 UTC in the NE eyewall. The new surface adjustment algorithms discussed previously were applied to this observation and produced a maximum 1-min sustained surface-adjusted (10 m) wind of 60 m s^{-1} (valid for marine exposure). The warm core–eyewall tilt adjustment was not required here because of the low flight level of this research mission, where the effects of thermal wind and surface friction are more closely balanced. The original Powell et al. (1996) methods produced a surface wind speed of 55 m s^{-1}, approximately 10% lower than this estimate. Records and avail-

[5] A complete listing of all surface wind analyses and plots of data coverage for Hurricane Donna is available at: http://www.aoml.noaa.gov/hrd/Storm_pages/donna1960/wind.html

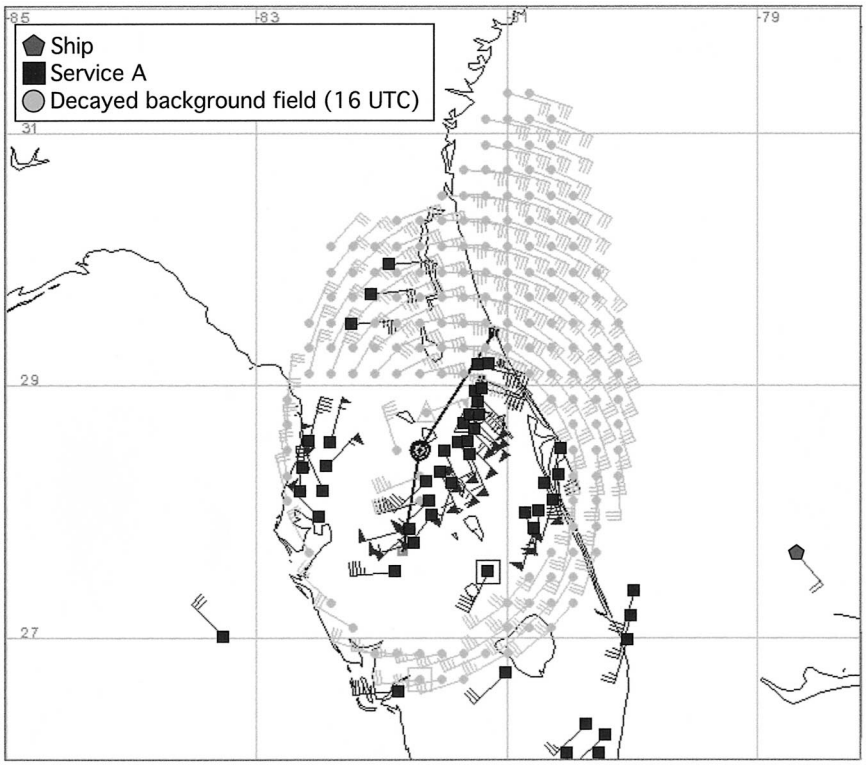

FIG. 11. The same as in Fig. 7 except for observations used in the postlandfall Hurricane Donna surface wind analysis for 0600 UTC 11 Sep 1960.

able in situ data indicated that Donna exhibited a fairly steady state of intensity during the next 6–8 h, which is reflected in the H*Wind analyses. A small increase in the eyewall radius beginning 0600 UTC 10 September 1960 was indicated in historical records (Tisdale 1960) and is reflected in the H*Wind analyses by a decrease in the highest 1-min wind speed between 1200 UTC and 1600 UTC on 10 September. This was associated with the strongest winds, which had been analyzed to be in the northeast quadrant, being positioned over land and weakening before the eye made landfall over southwest Florida.

Figures 7 and 8 show the available data used as H*Wind input for the 1800 UTC 9 September 1960 prelandfall and 1600 UTC 10 September 1960 landfall analyses conducted for Hurricane Donna. The NHRP surface-adjusted aircraft data indicated in Fig. 7 provided extensive in situ inner core wind measurements for the initial analysis. Unfortunately, this was the last flight into Donna to provide this kind of high-resolution data coverage. However, subsequent 6-hourly analyses did benefit from high-density background fields generated from the initial analysis. The use of background fields requires a somewhat steady-state tropical cyclone between analysis times. Kaplan (2002) showed that rapidly intensifying storms ($\geq$30 kt increase in intensity in 24 h) exhibited an average deepening of 4.6 m s^{-1} in 12 h. The average intensity change for that study's entire sample (1995–2000) of TCs was only 1 m s^{-1} in 12 h. A reasonable guideline for use of the background field in HRD analyses is that the TC intensity change during the previous 6 h should be $\leq$2.5 m s^{-1}. In order to promote the impact of the observations in the H*Wind analyses, the relative weight of the background field data was set to 0.1, as compared to in situ observations from lighthouses (1.0), surface land stations (1.0), aircraft (0.7), and ships (0.4). Figures 9 and 10 show a prelandfall and landfall surface wind analyses of Hurricane Donna, indicating its extensive impact along the southwest Florida coast. The radii of tropical storm force (17.5 m s^{-1}), 50 kt (26 m s^{-1}), and hurricane force (33 m s^{-1}) winds are indicated for each analysis and show a trend of decreasing over time.

d. Postlandfall surface wind analyses of Hurricane Donna

Four postlandfall surface wind analyses were made of Hurricane Donna beginning 1800 UTC 10 September and ending 1200 UTC 11 September 1960. These analyses posed logistical problems that related to the scarcity of wind data over land, particularly in Donna's core region. Aircraft reconnaissance and research flights typically do not fly over land regions, restricting the majority of available data to surface observing stations. Additionally, background fields developed to stabilize

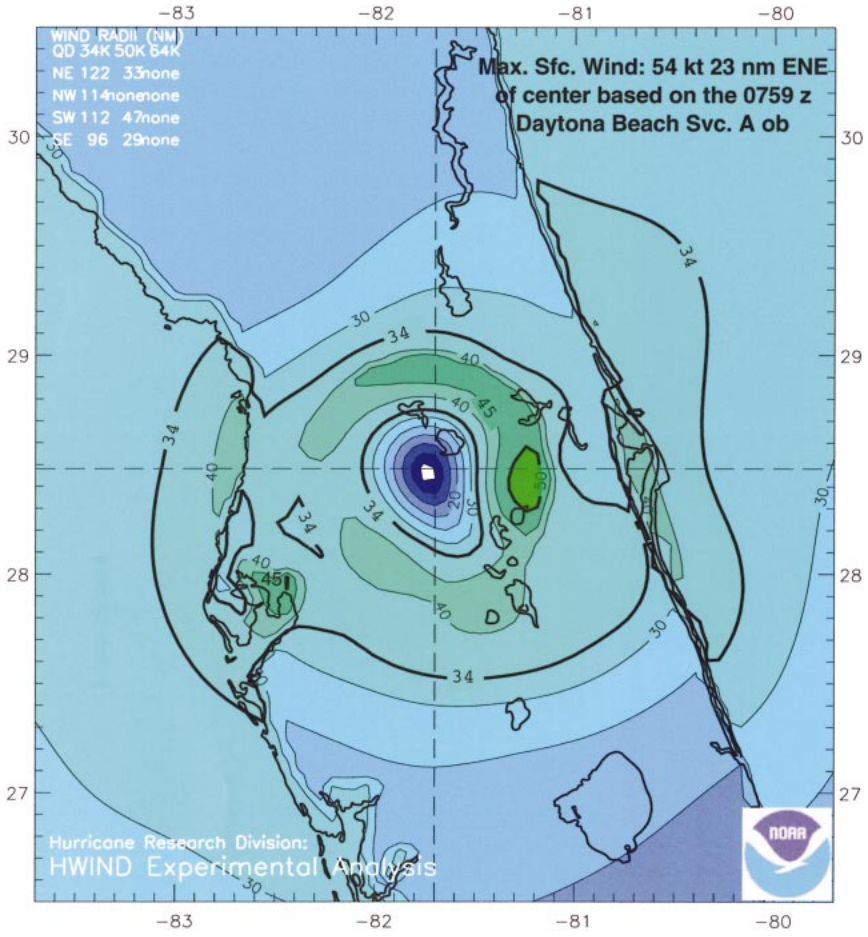

FIG. 12. Hurricane Donna postlandfall surface wind analysis for 0600 UTC 11 Sep 1960. Winds are max 1-min sustained 10-m surface winds (kt) valid for both marine and open terrain exposures. Significant wind radii are indicated in the upper-left corner. The analysis is based on adjusted background field data from the previous 1600 UTC analysis using the Kaplan–DeMaria Inland Wind Decay Model, as well as ship and Service A surface reports (0245–0959 UTC).

the marine analyses could not be utilized over land. The rapid decay that usually occurs after a storm has made landfall makes the use of these fields questionable. However, a method was developed to adjust the background field winds from their landfall values to the desired postlandfall analysis time using an inland wind decay model (IWDM). This allowed for a more representative wind field to be translated to the desired analysis coordinates.

The Kaplan–DeMaria IWDM provides an empirically based method for decaying tropical cyclone winds after landfall (Kaplan and DeMaria 1995). This model was designed to predict only the maximum sustained surface wind for a system after t h and is calculated by

$$V(t) = V_b + (RV_o - V_b)e^{-\alpha t} - C, \qquad (6)$$

where V_b is the background wind speed (kt) that the maximum 1-min landfall surface wind (10 m, marine exposure) decays to and is given as 26.7 kt (13.7 m s^{-1}), R is a frictional adjustment factor given as 0.9, V_o is the maximum 1-min sustained 10-m wind (≥30 kts/

TABLE 4. The same as in Table 3, except for postlandfall.

Date	MSLP (hPa)	Peak wind HURDAT (kt/m s^{-1})	Peak wind H*Wind (kt/m s^{-1})	RMW H*Wind (km)	34-kt radii NE/SE/SW/NW (km)	50-kt radii NE/SE/SW/NW (km)	64-kt radii NE/SE/SW/NW (km)
1800 UTC 10 Sep 1960	950	115/59	94/48	18	218/196/161/165	80/87/80/100	57/57/57/69
0000 UTC 11 Sep 1960	960	95/49	78/40	22	329/205/222/296	57/106/106/80	none/61/65/none
0600 UTC 11 Sep 1960	969	90/46	54/28	23	226/178/207/211	61/54/87/none	none
1200 UTC 11 Sep 1960	970	95/49	61/31	11	315/211/94/246	44/85/30/none	none

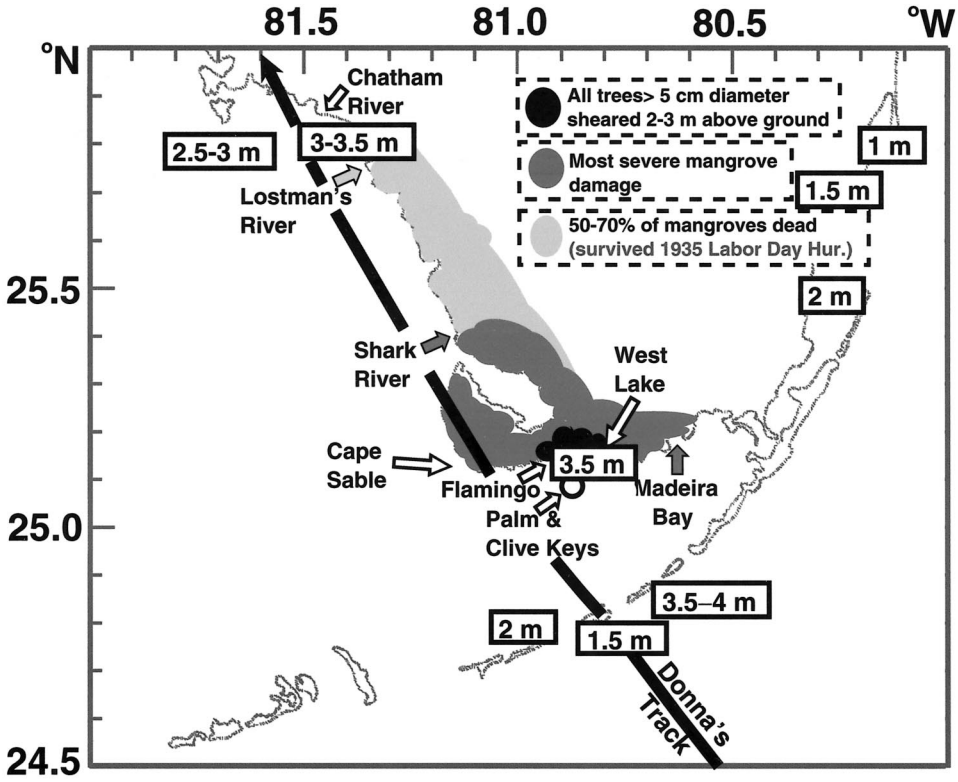

FIG. 13. Hurricane Donna's storm track and the associated storm surge and damage to flora experienced in southwest Florida (taken HP3).

15.5 m s^{-1}) with marine exposure at the time of landfall, α represents a decay constant, given as 0.095, t is time (h) after landfall, and C is a distance to land correction term that adjusts intensity by accounting for a storm center's proximity to the coastline after landfall (Kaplan and DeMaria 1995).

The application of the decay model to H*Wind background field data posed several challenges. First, the model uses a frictional decay constant (R) to account for the transition of a wind with marine exposure to one with open terrain exposure over land. However, H*Wind also performs this calculation, though in a more systematic manner. The coefficients used in Eq. (6) optimized the wind decay calculations, but necessitated a 10% boosting of the output wind be performed to compensate for the Kaplan–DeMaria model's overland adjustment. This allowed for overland adjustments to be made exclusively by the H*Wind system, producing more precise exposure corrections. Second, adjustments to the decay model scheme were necessary to allow the entire background field (composed of hundreds of wind vectors) to be utilized as model input, instead of simply using the single maximum wind at landfall. Background field winds from landfall were allowed to decay to magnitudes of no less than 30 kt (15.5 m s^{-1}) for this study. Though this was not the intended use of the Kaplan–DeMaria IWDM, they applied a similar technique to the landfall wind field of 1992 Hurricane Andrew (Kaplan and DeMaria 1995). The decay of the full landfall wind field to postlandfall times and positions provides a reasonable first guess wind field that is better than simply using the unadjusted landfall wind field. Finally, the distance to land correction (C) allows for the differentiating of decay rates for cases where the storm center makes landfall and skirts the coast versus those that make landfall perpendicularly to the coastline. This value was based on the distance of the center of circulation to the nearest coastal point at time t and was not calculated separately for each vector in the background field.

The surface wind field from Donna's 1600 UTC landfall on 10 September 1960 (Fig. 10) was used to create the background field that was utilized by the Kaplan–DeMaria IWDM. These winds were decayed out to various postlandfall times and repositioned in storm relative coordinates based on the new storm center location. The decayed background field data compared well with available in situ data, as shown in Fig. 11, though some background field wind vectors that were inconsistent with in situ observations were omitted from the analyses. Figure 12 shows the 0600 UTC 11 September 1960 H*Wind postlandfall analyzed wind fields for Donna and indicate a relatively rapid decay of the system as it passed over the Florida peninsula. As indicated by Table 4, there were more substantial discrepancies between the HURDAT and H*Wind analyzed intensities during the postlandfall time period. It is important to note that

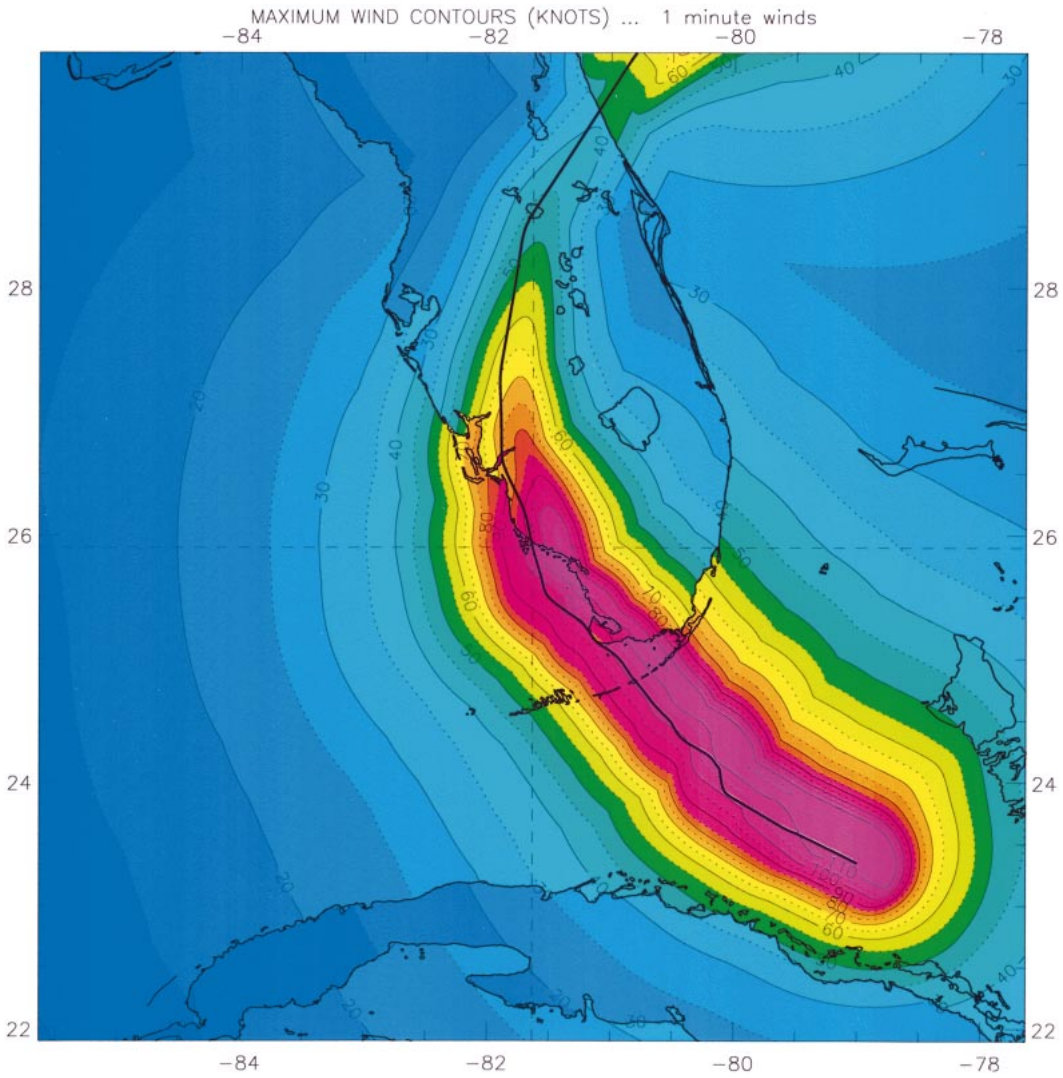

FIG. 14. Swath of peak max 1-min sustained winds (kt) experienced along Hurricane Donna's track (black curve). Winds are max 1-min sustained 10-m surface winds valid for marine and open terrain exposures.

H*Wind provides a lower bound of storm intensity, since it cannot produce winds that are stronger than were observed. This is particularly significant in cases where the maximum winds in a given storm are not adequately sampled. However, none of the available postlandfall observations in the inner core region of Donna or in poststorm reports collected by Dunn (1961) support the strong category-2 status that is maintained in HURDAT (Fig. 11).

Prior to 1967, HURDAT has been shown to exhibit several weaknesses in its description of both track and intensity. Neumann (1994) points out that before 1957, tropical cyclone positions were only estimated twice per day (0000 and 1200 UTC) and were needed at 6-hourly intervals for entry into HURDAT. However, he also noted that some of these records were missing from the period between 1955 and 1966, forcing the use of an intermediate linear interpolation scheme for determining wind speed (Akima 1970). This scheme was used to calculate the intermediate positions, regardless of a storm's location over land or water. Particularly over land, interpolations do not sufficiently describe the rapid decay that often occurs with landfalling tropical cyclones. It is of interest to note that intensity estimates for Donna by HURDAT and H*Wind both show that this storm began a period of reintensification between 0600 and 1200 UTC 11 September 1960 after it exited the Florida peninsula. Therefore, an interpolation calculation between the 0000 and 1200 UTC intensity estimates would likely result in a high biased 0600 UTC intensity estimate. Additionally, Neumann (1994) noted a consistent bias in HURDAT that resulted in an insufficient decrease in wind speeds after landfall. Landsea (1993) also indicated that Atlantic major hurricanes during the 1940s through the 1960s were overestimated in wind intensity (relative to observed central pressure)

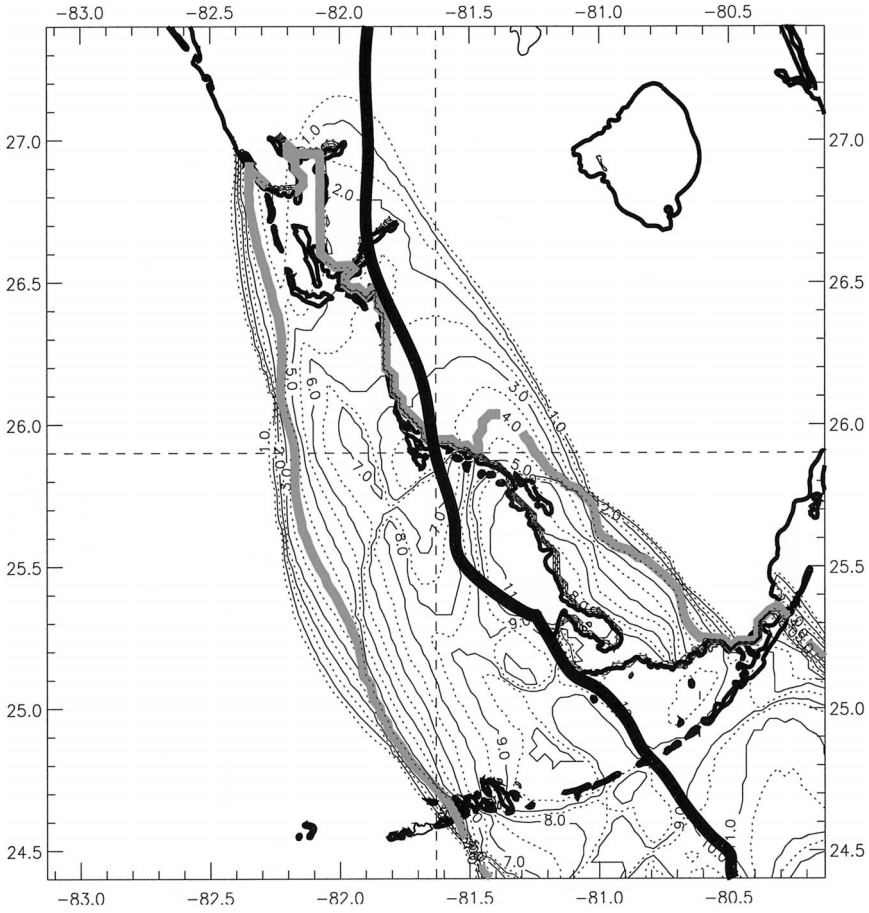

FIG. 15. Swath of duration (h) of hurricane-force and greater (≥33 m s^{-1}) winds experienced along Hurricane Donna's track (black curve). The calculation was based on max 1-min sustained 10-m surface winds valid for marine and open terrain exposures. The 4-h duration contour is indicated by the gray curve.

by an average of 5–10 kt (2.5–5 m s^{-1}). These problems inherent in the HURDAT dataset are possible causes for the discrepancies seen in Table 4.

e. Parameterization of tropical cyclone impact

Figure 13 was taken from HP3 and shows Hurricane Donna's track and the associated storm surge and local damage to flora experienced in southwest Florida. Maximum surges of 3.5–4 m were recorded in the middle keys and severe to complete damage to mangrove forests was documented. Swaths of peak winds experienced along the storm track were created and indicate areas of high wind damage susceptibility. Figure 14 shows this parameter for Hurricane Donna and suggests that category-4 (at least 58.5 m s^{-1}/111 kt) winds occurred in the middle Florida Keys and 58.5 m s^{-1}/111 kt winds affected the immediate southwest Florida coastline near Cape Sable. A broad region between Madeira Bay and Cape Sable and northward to Fort Myers Beach experienced peak winds of ≥49 m s^{-1}/96 kt (category 3). This vast swath of category-3 winds fell generally along unpopulated regions in 1960, although the population today in the Florida Keys and Naples region is much larger. Category-1 winds extended from Boca Chica Key northeast to Key Largo and northward along Florida's southwest coast to Cape Coral.

Although highest sustained wind speeds are certainly an important factor when examining damage induced by a tropical cyclone, there are other significant parameters to consider. Figures 15 and 16 show swaths of duration (h) of hurricane (≥33 m s^{-1}) and major hurricane-force (≥49 m s^{-1}) winds experienced along Donna's track, respectively. This parameter inherently describes the repeated loading and unloading of gusts and lulls in a turbulent wind field, which directly impact structural damage (Powell et al. 1995). Figure 15 shows that hurricane-force winds affected the northern coast of Florida Bay near Flamingo for up to 9 h and Fig. 16 indicates that major hurricane–force winds were experienced for up to 4.5 h. Nearly all of the Florida Keys from Sugerloaf Key to Key Largo experienced hurricane-force winds for more than 4 h and major hurricane–force winds for at least 2 h. The longer a region ex-

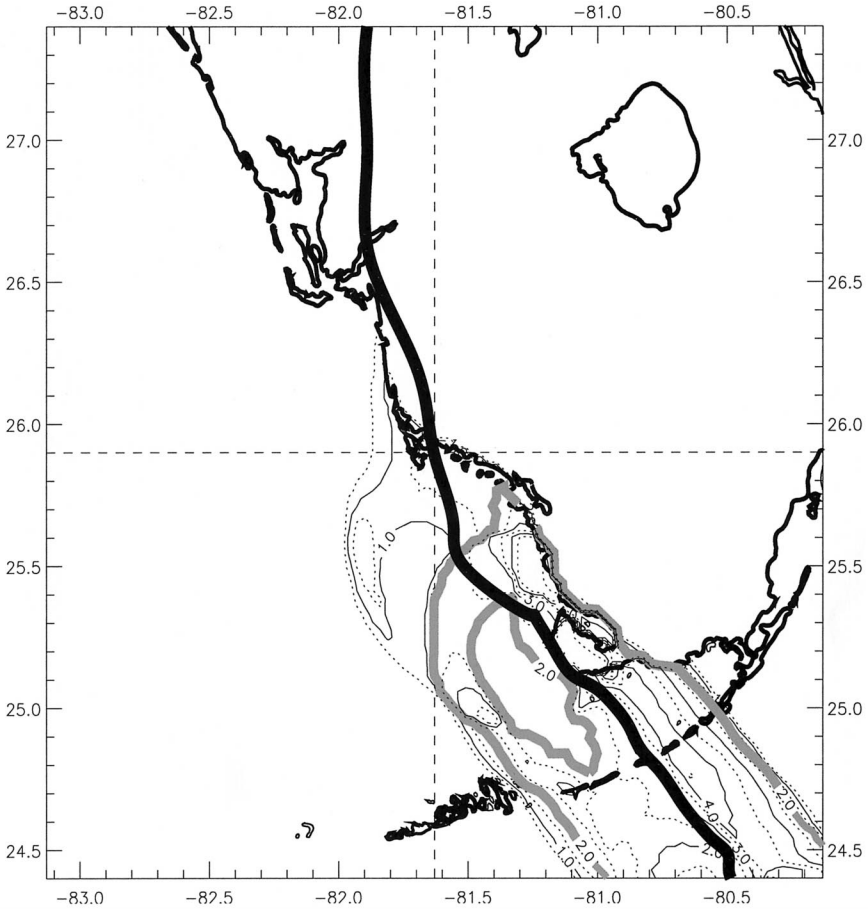

FIG. 16. Swath of duration (h) of major hurricane–force (≥49 m s^{-1}) winds experienced along Hurricane Donna's track (black curve). The calculation was based on max 1-min sustained 10-m surface winds valid for marine and open terrain exposures. Dashed contours indicate 0.5-h intervals. The 2-h duration contour is indicated by the gray curve.

periences hurricane- and especially major hurricane–force winds, the more extensive the damage that can be experienced. The largest values of duration shown in Figs. 15 and 16 correspond to the areas of maximum environmental damage indicated in Fig. 13.

Steadiness is defined by the ratio of the vector mean wind to the scalar mean wind over the time period required for a storm to traverse a region (Powell et al. 1995). The lowest values of steadiness are characteristic for areas that experience the rapid changes in wind direction associated with the passage of the tropical cyclone circulation center. This parameter provides a means of quantifying the damaging effects caused by extreme shifts of wind direction on local structures and vegetation. Figure 17 is a plot of steadiness along Donna's track and shows that areas of low steadiness (<0.4) were associated with the areas of large-scale damage indicated in Fig. 13. This was also found by HP3.

Parameterization of the effects of tropical cyclone wind fields can be effectively quantified by swaths of peak winds, wind steadiness, and duration of hurricane- and major hurricane–force winds. The damage swath indicated in Fig. 13 appears to be coincident with the areas of maximum intensity and duration of winds, as well as the minimum values of steadiness associated with Hurricane Donna. These products offer the ability to evaluate the damage associated with tropical cyclones, as well as assess damage potential.

4. Discussion

The reanalysis of Hurricane Donna using an objective surface wind analysis application such as H*Wind sets initial groundwork for reconstructing some of the twentieth century's most powerful landfalling Atlantic hurricanes. Because these analyses utilize real data and are not simply derived through parametric modeling, they offer improved descriptions of a hurricane's wind field, when provided sufficient observations. By using all available in situ wind data, comprehensive analyses can be constructed to help identify weaknesses in the HURDAT archive, complimenting current work by Landsea

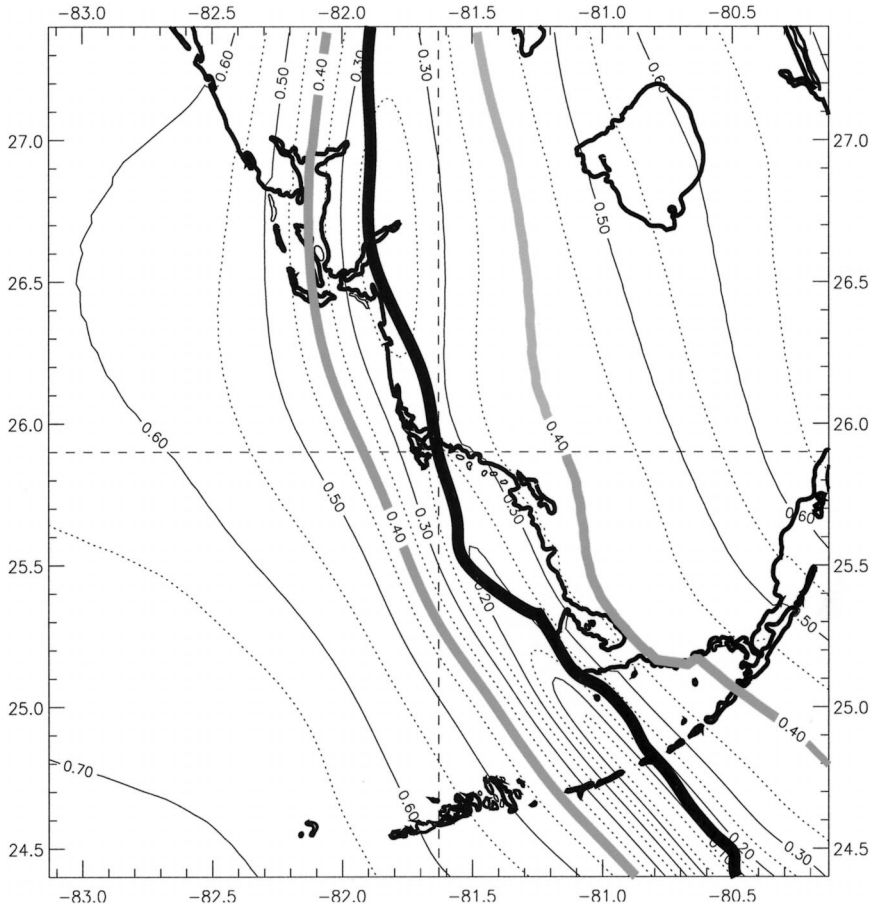

FIG. 17. Swath of wind steadiness experienced along Hurricane Donna's track. Donna's track and the 0.4 wind steadiness contours are indicated by the black and gray curves, respectively.

et al. (2003). An accurate analysis of surface winds in major hurricanes like Donna not only provides a method for improving historical records, but can also be utilized by insurers to examine potential financial liabilities associated with these storms. The extreme damage caused by Hurricane Andrew in 1992 (an estimated $26.5 billion total) exemplifies the importance for insurers to accurately assess the level of risk in various coastline communities. Descriptions of peak winds, duration of hurricane- and major hurricane–force winds, and wind steadiness associated with Hurricane Donna provide an additional means of specifying storm damage potential and correlating losses for a given along-track region.

Future plans associated with this work include integrating the new aircraft-to-surface adjustment algorithms developed here into real-time operations (Dunion and Powell 2002). Also, stratifications of GPS sonde wind profiles based on stability in the boundary layer, vertical shear variation, and storm quadrant are planned and may further improve the algorithms for the surface reduction of aircraft flight-level winds. Since relatively few numbers of GPS sonde observations exist in >70 m s^{-1} tropical cyclone environments, attempts will be made to expand the current database for these high-wind cases as new aircraft and GPS data become available. Finally, the continuation of data acquisition and wind field construction of several more category-4 and -5 hurricanes that affected the U.S. coast during the twentieth century is planned. This would help further our understanding of the potential financial risks associated with landfalling catastrophic hurricanes.

5. Summary and conclusions

The following include findings and recommendations related to conclusions drawn from this study:

- A warm core–eyewall tilt algorithm was developed for application to the surface adjustment of aircraft flight-level winds. This algorithm can be used to more accurately equate reconnaissance aircraft winds to mean boundary layer winds (0–500-m average).
- A new algorithm is presented to optimize the adjustment of mean boundary layer winds to equivalent surface winds in high wind speed regimes (MBL winds > 55 m s^{-1}).

- The Kaplan–DeMaria Inland Wind Decay Model was integrated into HRD's surface wind analysis system for the first time and provided low-weighted background field wind data for postlandfall Donna analyses.
- Analyses of peak maximum sustained winds associated with Hurricane Donna indicate that category-4 (winds $\geq$ 58.5 m s^{-1}) affected the middle Florida Keys and that a broad swath of category-3 (winds $\geq$ 49 m s^{-1}) was experienced from Maderia Bay to Cape Sable, northward to Fort Myers Beach, Florida.
- Analyses of duration of hurricane- and major hurricane–force winds associated with Hurricane Donna indicate that these winds were experienced along the southwestern Florida coastline for up to 9 and 4.5 h, respectively.
- Analyses of wind steadiness along Hurricane Donna's track indicate that a vast region of the Florida Keys and the southwestern Florida peninsula experienced values of <0.4, indicating highly variable wind directions and large damage potentials.
- Based upon results shown by this work, changes to HURDAT's Hurricane Donna archive are recommended. Reductions in the peak maximum 1-min winds are particularly warranted after landfall.

Acknowledgments. This study was supported by the Risk Prediction Initiative of the Bermuda Biological Station and supplemented by additional funding from the Insurance Friends of the National Hurricane Center. The authors would like to thank John Kaplan of HRD for his assistance integrating the Kaplan–DeMaria Inland Wind Decay Model into the HRD surface analyses. Special thanks to James Franklin for insightful input into the surface adjustment algorithm development and interpretation of the GPS sonde data, as well as Mike Black and Steve Feuer for their assistance in postprocessing many of the GPS sondes used in this study. George Soukup also of HRD was instrumental in the development of the programs that were used to generate the various damage swaths used in this work.

REFERENCES

Akima, H., 1970: A new method of interpolation and smooth curve fitting based on local procedures. *J. Assoc. Comput. Mach.,* **17,** 589–602.

Charnock, H., 1955: Wind stress on a water surface. *Quart. J. Roy. Meteor. Soc.,* **81,** 639–640.

Cione, J. J., P. G. Black, and S. H. Houston, 2000: Surface observations in the hurricane environment. *Mon. Wea. Rev.,* **128,** 1550–1561.

Doane, D. C., 1985: *Time Changes in the USA.* American Federation of Astrologers, Inc., 198 pp.

Dunion, J. P., and M. D. Powell, 2002: Improvements to the NOAA Hurricane Research Division's surface reduction algorithm for inner core aircraft flight-level winds. Preprints, *25th Conf. on Hurricanes and Tropical Meteorology,* San Diego, CA, Amer. Meteor. Soc., 581–582.

——, and C. S. Velden, 2002: Application of surface-adjusted GOES low-level cloud-drift winds in the environment of Atlantic tropical cyclones. Part I: Methodology and validation. *Mon. Wea. Rev.,* **130,** 1333–1346.

Dunn, G. E., 1961: The hurricane season of 1960. *Mon. Wea. Rev.,* **89,** 99–107.

Franklin, J. L., S. J. Lord, S. E. Feuer, and F. L. Marks, 1993: The kinematic structure of Hurricane Gloria (1985) determined from nested analyses of dropwindsonde and Doppler data. *Mon. Wea. Rev.,* **121,** 2433–2451.

——, M. L. Black, and K. Valde, 2000: Eyewall wind profiles in hurricanes determined by GPS dropwindsondes. Preprints, *24th Conf. on Hurricanes and Tropical Meteorology,* Ft. Lauderdale, FL, Amer. Meteor. Soc., 446–447.

Goodberlet, M. A., C. T. Swift, and J. C. Wilkerson, 1989: Remote sensing of ocean surface winds with the Special Sensor Microwave/Imager. *J. Geophys. Res.,* **94,** 14 547–14 555.

Hawkins, H. F., and D. T. Rubsam, 1968: Hurricane Hilda, 1964: II. The structure and budgets of the hurricane on October 1, 1964. *Mon. Wea. Rev.,* **96,** 427–434.

Hock, T. F., and J. F. Franklin, 1999: The NCAR GPS dropwindsonde. *Bull. Amer. Meteor. Soc.,* **80,** 407–420.

Houston, S. H., and M. D. Powell, 2003: Surface wind fields for Florida Bay hurricanes. *J. Coastal Res.,* in press.

——, P. P. Dodge, M. D. Powell, M. L. Black, G. M. Barnes, and P. S. Chu, 2000: Surface winds in hurricanes from GPS-sondes: Comparisons with observations. Preprints, *24th Conf. on Hurricanes and Tropical Meteorology,* Ft. Lauderdale, FL, Amer. Meteor. Soc., 339.

Jarvinen, B. R., C. J. Neumann, and M. A. S. Davis, 1984: A tropical cyclone data tape for the north Atlantic basin, 1886–1983: Contents, limitations, and uses. NOAA Tech. Memo. NWS NHC 22, Miami, FL, 21 pp.

Kaplan, J., 2002: Estimating the probability of rapid intensification using the SHIPS model output: Some preliminary results. Preprints, *25th Conf. on Hurricanes and Tropical Meteorology,* San Diego, CA, Amer. Meteor. Soc., 124–125.

——, and M. DeMaria, 1995: A simple empirical model for predicting the decay of tropical cyclone winds after landfall. *J. Appl. Meteor.,* **34,** 2499–2512.

Katsaros, K. B., E. B. Forde, P. Chang, and W. T. Liu, 2001: QuikSCAT's SeaWinds facilitates early identification of tropical depressions in 1999 hurricane season. *Geophys. Res. Lett.,* **28,** 1043–1046.

Landsea, C. W., 1993: A climatology of intense (or major) Atlantic hurricanes. *Mon. Wea. Rev.,* **121,** 1703–1713.

——, and Coauthors, 2003: The Atlantic Hurricane Database Reanalysis Project—Documentation for 1851–1910 alterations and additions to the HURDAT Database. *Hurricanes and Typhoons: Past, Present, and Future,* R. J. Murnane and K. B. Liu, Eds., Columbia University Press, in press.

Marks, F. D., R. A. Houze Jr., and J. F. Gamache, 1992: Dual-aircraft investigation of the inner core of Hurricane Norbert. Part I: Kinematic structure. *J. Atmos. Sci.,* **49,** 919–942.

Miller, B. I., 1963: On the filling of tropical cyclones over land. National Hurricane Research Project Rep. 66, Miami, FL, 82 pp.

——, 1964: A study of the filling of Hurricane Donna (1960) over land. *Mon. Wea. Rev.,* **92,** 389–406.

Neumann, C. J., 1994: An update to the National Hurricane Center ''Track Book.'' *Minutes of the 48th Interdepartmental Conf.,* Miami, FL, NOAA/Office of Federal Coordinator for Meteorological Services and Supporting Research, A-47–A-53.

OFCM, 2002: National hurricane operations plan. Publ. FCM-P12-2002, 159 pp. [Available from the Office of the Federal Coordinator for Meteorological Services and Supporting Research, Suite 1500, 8455 Colesville Rd., Silver Spring, MD 20910.]

Ooyama, K. V., 1987: Scale controlled objective analysis. *Mon. Wea. Rev.,* **115,** 2479–2506.

Pielke, R. A., Jr., and R. A. Pielke Sr., 1997: *Hurricanes: Their Nature and Impacts on Society.* John Wiley and Sons, 279 pp.

——, and C. W. Landsea, 1998: Normalized hurricane damages in the United States: 1925–95. *Wea. Forecasting,* **13,** 621–631.
Powell, M. D., and P. G. Black, 1990: The relationship of hurricane reconnaissance flight-level measurements to winds measured by NOAA's oceanic platforms. *J. Wind Eng. Ind. Aerodyn.,* **36,** 381–392.
——, and S. H. Houston, 1996: Hurricane Andrew's landfall in south Florida. Part II: Surface wind fields and potential real-time applications. *Wea. Forecasting,* **11,** 331–349.
——, ——, and I. Ares, 1995: Real-time damage assessment in hurricanes. Preprints, *21st Conf. on Hurricanes and Tropical Meteorology,* Miami, FL, Amer. Meteor. Soc., 500–502.
——, ——, and T. A. Reinhold, 1996: Hurricane Andrew's landfall in south Florida. Part I: Standardizing measurements for documentation of surface wind fields. *Wea. Forecasting,* **11,** 304–328.
——, ——, L. R. Amat, and N. Morisseau-Leroy, 1998: The HRD real-time hurricane wind analysis system. *J. Wind Eng. Ind. Aerodyn.,* **77/78,** 53–64.
——, T. A. Reinhold, and R. D. Marshall, 1999: GPS sonde insights on boundary layer wind structure in hurricanes. *10th International Conference On Wind Engineering,* A. Larsen, G. L. Larose, and F. M. Livesey, Eds., A. A. Balkema Publishers, 307–314.
Thompson, E. F., and V. J. Cardone, 1996: Practical modeling of hurricane surface wind fields. *J. Waterw. Port Coastal Ocean Eng.,* **122** (4), 195–205.
Tisdale, C. F., 1960: The weather and circulation of September 1960. *Mon. Wea. Rev.,* **88,** 353–361.
U.S. Department of Energy, 1978: National wind data index final report. Rep. HEO-T1041-01, 198 pp.
Vickery, P. J., and L. A. Twisdale, 1995: Wind-field and filling models for hurricane wind-speed predictions. *J. Struct. Eng.,* **121,** 1700–1709.